Journal of Engineering and Sustainable Developmen
http://jeasd.uomustansiriyah.edu.iq/index.php
https://doi.org/10.31272/jeasd.25.2.6

JEASD

Vol. 25, No02, March 2021
ISSN 2520-0917

INVESTIGATIVE STUDY OF THERMAL PERFORMANCE OF THERMOSYPHON SOLAR COLLECTOR

*Ayoob K. Jasim[1] Basim H. Abbood[1] Mohammed H. Alhamdo[1]

1) Mechanical Engineering Department, College of Engineering, Mustansiriyah University, Baghdad, Iraq

Received 14/10/2020 ***Accepted in revised form 26/10/2020*** ***Published 1/3/2021***

Abstract: Experimental and Numerical investigation has been performed to improve the thermosyphon thermal performance. Optimization process concentrated on both the water and the operating liquid temperature inside the tank and the thermosyphon. For this purpose, three different models of improvement methods have been studied that depend on increasing the surface area with no changing in the volume of operating liquid. The first one (case-A-) is by add ten ring fins about the absorber pipe. The second method (case-B-) is by add twenty ring fins about the absorber pipe. While, the third way (case-C-) is by add ten ring fins with ten grooves about the absorber pipe. The thermosyphon thermal performance was compared between the traditional model and experimental model. Moreover, numerical simulate for all cases were done with computational fluid dynamic (CFD), ANSYS 19.R3. It was observed through the results that a good convergence between the numerical and, experimental results. Furthermore, the thermal performance for case-A- is found greater than all other cases under study.

Keywords: *Natural Convection, Thermosyphon, Thermal Performance, Ring Fins, CFD.*

1. Introduction

There are several types of the renewable energy sources [1], however the most significant of renewable energy sources is solar energy due to available in abundance universal [2]. One of the most systems that used sunlight to heat water is a thermosyphon solar collector. Several tries have conducted to develop the thermosyphon design to obtain a superior thermal performance. A numerical study by computational fluid dynamics to compare between the conventional and, helical model, with mutable number of cycles 10, 20 and 30 to enhance the thermal performance was conducted through (Freegah et al., 2014) [3]. They have proven that the usage of helical riser pipe conduct to a major enhancement of a theromsyphon performance compared to conventional model. Furthermore, temperature of the heat exchanger was increased due to increasing the turns number of helical pipes. While, increasing the number of helical pipe does not improve the theromsyphon performance. (Manjunath M. S. et al., 2011) [4] Presented a numerical analysis study to improve the heat transfer process of flat plate solar collector. They have studied the effect of used fined tube namely serrated fins and planar fin on the flat plat collector performance. The finding data indicated that the heat transfer process increased for proposal model compared to the conventional model. Mutable cross-section area of the absorption pipe of the solar water heater has been verified experimentally by (Pankaj N. Shrirao et al., 2018) [5]. The effect of two shapes of absorbent pipe namely cylindrical and airfoil shape on the solar collector thermal efficacy has been investigated. They recorded that the airfoil absorber tubes gained large amount of

*Corresponding Author: ayoobkhalid411@gmail.com

solar radiation compared to the other absorber tube. Hence, the efficiency of the airfoil-shaped absorption tube improved by 10 to 12% as compared with circular shape of absorbent pipe. (M. Balachandar and A. Narendran, 2016) [6] analyzed experimentally the flow of fluid also the heat transmission of flat plate collector. The impact of internal grooves inside absorbent pipe of the solar collector device on the heat transfer properties has been examined. They have reported that the flat plate collector efficiency improved by 5% for used proposal collector compared to traditional collector. (H. Hussein et al., 2006)[7] Presented an experimental study to improve the flat plate collector performance. They have examined the influence of wickless heat pipe geometry and, operating liquid filling ratio on the flat plate collector performance. Three cross-section geometry are circular, elliptical and semicircular have been used. Each group charged with three different filling ratio 10%, 20% and 35% with variable inlet cooling water temperature and mass flow rate under the condition of Cairo, Egypt. The results shown that the elliptical cross section geometry with law water filling ratio of 10% was better compared to other types. (Jayesh V. Bute and S.C. Kongre, 2016) [8] Conducted an experimental study to improve the heat absorption for solar collector. The effect of variable the absorber pipe shapes namely straight and zig-zag on both heat transmission process and thermal behaveor has been examined. They reported that quantity of heat transfer was higher for zig-zag model compared to straight model. In addition, the zig-zag absorber pipe recorded increase Nusselt number by 18.91% compared to straight pipe. (Keguang Yao et al., 2015) [9] Evaluated the heat transmission and flow performances of solar collection device using CFD simulation. They were study the influence of used twist tape with different primary temperature on the solar collectors' heat transmission process. They reported that the combination of operating liquid close the surface further intensive and generate further swirls also reduce the fluid speed this makes better heat transfer. Furthermore, the thermal performance enhancement of solar collector with relative twisted ratio of the twist tape =2.5m and 4m is higher by 1.07% and 9.29% respectively than conventional collector. The flat plate collector thermal performance was experimentally conducted with (R. Herrero Martin et al., 2011) [10]. The impact of usage wire coils in the absorber tubes to enhance heat transmission and solar absorption has been examined. They have indicated that the efficiency increase with wire coils insert as compare with the standard collector. Moreover, the heat transfer improve of the enhanced collector is due to reducing the thermal losses by 30%. (Rohit Khargotra et al., 2017) [11] conducted a compare between variable tabulators' on the performance of solar collection device. Clarify experimentally the impact of usage coil-spring and twist tape within the absorbent tube on the thermal efficiency and heat transmission of solar collection system. They reported that the maximum efficiency in term of operating liquid temperature at exit of the absorber and heat transfer coefficient was for twisted tape turbulator of 63%. (Chandresh Sharma and Rajendra Karwa, 2014) [12] Conducted an experimental study to improved solar collection system performance. The influence of used 75% of the twisted section as insertion device to improve heat transmission and enhanced the thermal efficiency of the thermosyphon has been examined. They have been indicated rise in the thermal efficacy of solar collector by 4.5-8% due to the usage of the 75% twisted tape as insertion tool. (Braa Khalid Ameen et al., 2015) [13] Carried out several trials to increase the heat transmission

of the solar collection device for Iraqi climatologic environments. Compared study of different types of insertion single twisted tape (STT), double twisted tape (DTT) and mixed twisted tape (MTT) in the absorbent tube with different number of glazing as well as different number of Reynolds number has been done. Based on the obtained results, double twist tape provides a huge positive influence than the other types of insertion through rise of the outlet operating liquid temperature. (Alireza Hobbi and, Kamran Siddiqui, 2009) [14] Tested the thermal performance of SWHs experimentally. The effect of various types of insertion namely twist tape, coil spring wire, and conical ridges have been studied on the system efficiency. They have reported that all types have improved thermal performance compared with traditional model. While, there is no significant difference of heat transfer among proposal types under study. However, numerical and experimental examinations of thermal performance in terms of the temperature of the water within the storage container and the operating liquids at the entrance and exit of the absorber tube can provide a good indicator regarding the design conditions of the thermo-siphon system. The unsteady state has not been analyzed and maintained on the same volume of operating liquid compared to the conventional model in a thermo-siphon device with an adequate variety of absorber tube shapes. Thus, the current study trying to fill these research gaps by analyzing three different models. Model -A- In the present model, the exposed surface area to heat flow is rised by add ten ring fins about the absorption tube. While in the model-B- the exposed surface area to heat flow is rised by add twenty ring fins about the absorption tube. However, in the model-C- the exposed surface area to heat flow is rised by add ten ring fins with ten grooves about the absorption tube.

2.1 Experimental Work

The current section provides brief description about the rig components and the measuring device specification which used in this study. Experimental test were conducted in the winter season in Baghdad (33.3ON and 44.3 OE). The test device consists of one absorption pipe and a 9.4 liter storage tank as well as a heat exchanger that passes within the tank in order to exchange heat between the operating liquid and water inside the tank, as well as five thermocables with a temperature recorder in order to measure the temperature of water and operating liquid while the intensity of solar radiation is measured using a solar power meter. Furthermore, the test device components can be clearly seen in figure (1), as well as table (1) consider all device specifications for the presents study.

Table 1. Test device specifications under current work

Item	Dimension or material
Height of thermo-siphon device	1.2m
Width of thermo-siphon device	0.6m
The slope angle of collector	33º
Number of absorber tubes	1m
The absorber tube length	1m
Inner diameter of the absorber tube and down-comer	0.01446m
Outer diameter of the absorber tube and down-comer	0.01588m
Material of the absorber tube	Copper
The tank diameter	0.2m
The tank high	0.3m
The material of tank	Plastic
Rubber plastic sponge insulation thickness	0.01m

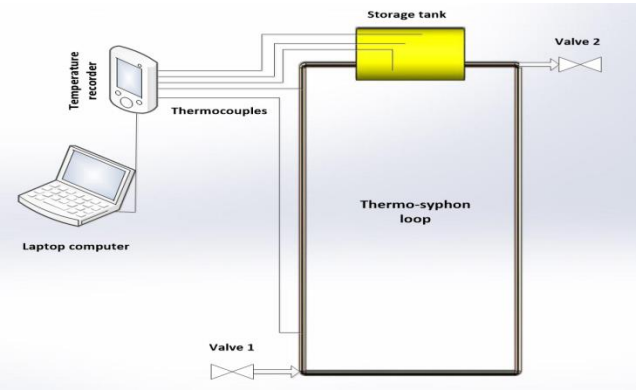

Figure 1. Diagram viewer of thermosyphon device.

2.2 Experimental Setup

The solar collector used in this study consists of one absorber pipe with outer diameter, thickness, and length of 15.88 mm, 0.71 mm, 1000 mm, respectively, as for the recirculating pipe has a thickness and an outer diameter similar to the absorption pipe. Moreover, a temperature recorder (BTM-4208SD\12 channels) with five thermocouples type K was used to measure the operating liquid temperature at both the entrance and exit of the absorption tube and measure the temperature of water in the container, also a solar power meter (TES1333R) was usage to measure the intensity of solar radiation as shown in the figure (2).

Figure 2. Photo of the thermo syphon device.

3. Numerical Computation

In the present study, the geometrical model done with the numerical simulation using computational fluid dynamics method, ANSYS R 19.R3. Usually, analysis of geometrical model by using (CFD) passes with three main steps. The first step contains build and mesh generation of the geometrical model. While the second step denotes determine boundary conditions of geometrical model. The last step is dedicated to presenting results.

3.1 Geometric Modeling

In the current work, four structures of thermosyphon device namely: traditional model, add ten ring fins about the absorption tube (case-A-), add twenty ring fins about the absorption tube (case-B-) while the last model that consist of ten ring fins with ten grooves about the absorption pipe (case-C-). The test device consists of a single absorption pipe that absorbs the heat flux and transfers it to the operating liquid, which is transferred by the effect of the density difference to the heat exchanger that passes inside the tank where the heat exchange process occurs between the operating liquid and water, after which the operating liquid returns through the recirculating pipe which has same diameter and thickness of absorption pipe. The test device height of 1200 mm, width of 600 mm, and tilted angle of a 33 ° while the absorber tube specifications of the of all cases can be offered as below.

Conventional model: The outer diameter and thickness of the absorption tube are (15.86 mm) and (0.71 mm) respectivily as shown in figure (3a).

Case-A-: The absorption tube dimensions are similar of conventional model. Moreover, ring fins are add to the absorption tube with inner, outer diameter and thickness are (15.88 mm), (27.6 mm) and (0.71mm) respectively as shown in figure (3b).

Case –B- The absorber tube dimensions are same dimensions of case –A-. Furthermore, twenty ring fins to the absorber tube were add with inner diameter, outer diameter and thickness are (15.88mm), (22.5 mm) and (0.71mm) respectively.

Case –C- The absorber tube dimensions are same dimensions of case –A-. Furthermore, ten ring fins to the absorber tube were add

with inner diameter, outer diameter and thickness are (15.88mm), (22.5 mm) and (0.71mm) respectively. As well as ten groove to the absorber tube were added with inner diameter, outer diameter and thickness are (15.08mm), (15.88mm) and (7.6mm) respectively.

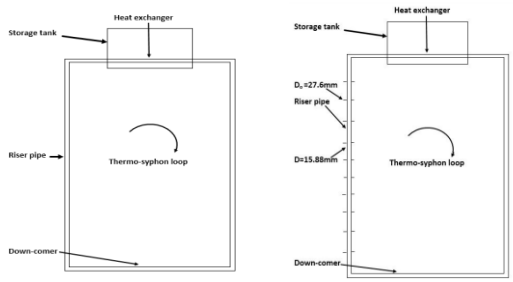

a **b**

Figure 3. Thermo syphon geometry (a) Traditional model and (b) Case-A-.

3.2. Mesh Generation

The engineering mesh has a great influence on the results accuracy of numerical simulations. Therefore, in the current study, a hexahedral grid is used to mesh the engineering models field. This type of mesh is characterized by providing more accurate results and needs less storage memory, as well as the high ability to connect several complex geometric shapes [15]. The below figure demonstrated the hexagonal grid shape of the test model.

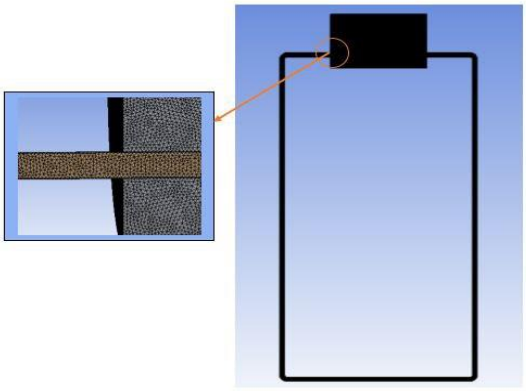

Figure 4. Geometry mesh domain

3.3. Boundary Conditions

The boundary conditions which are usage with all models in the present numerical simulation study are the initial temperature for the water and the operating liquid is 23°C, (9.4 L) of water in the tank also (0.95 L) of the operating liquid inside the thermo-siphon. Moreover seven hours of transient heat flux as depicted in figure (5) was applied on the absorber pipe which can be calculated by Equation (1) [16]. In addition, used user-defined function (UDF) to enter the values of hear flux into computational fluid dynamic Ansys fluent. As well as, water used as operating liquid with density, viscosity, specific heat, thermal conductinty and thermal expansionrate are 998.2 kg / m3, 0.001003 kg / (m.s), 4182 J / kg-K, 0.6 W/m-K and 0.000149K-1 while for copper pipe density, specific heat, thermal conductinty are 8978 kg / m3, 381 J / kg-K and 386 W/m-K.

$$q = I_T \varepsilon \tau [\sin\delta \sin(\theta - \propto) + \cos\delta \cos(\theta - \propto) \cos\omega] \quad \ldots(1)$$

where I_T, δ, θ, $\propto$, τ and ω represent intensity of solar radiation, the slope of thermo-siphon device, local latitud, transmission of atmosphere and the sun hour angle respectively. While, ε denote the earth's orbit correction factor that could calculated by Eq. (2) [17].

$$\varepsilon = (1 + 0.033 \cos((360N\_d)/365)) \quad \ldots(2)$$

Where N_d are denote number of the day of the year

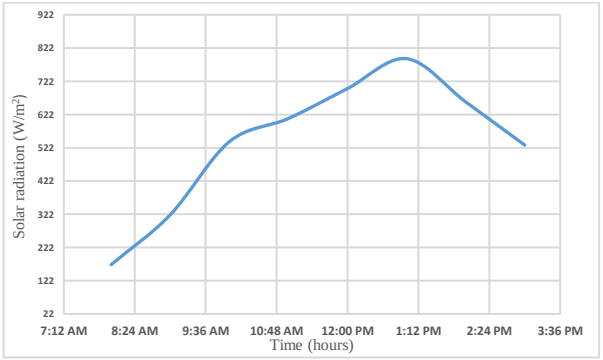

Figure 5. Variation of solar radiation for seven hours.

3.4. Principal Equations

In the present research, the 3D Navier-Stokes relationships, continuity equation and, the energy equation were numerically explained to simulate the transient flow and the water

temperature within the storage tank, operating liquid at the outlet and inlet of the absorber tube for the thermo-siphon for seven hour of effective time. Bellow some assumptions are considered under the current study.

The operating liquid that stream within the thermosyphon device is water.

The stream is single phase, laminar and steady state also compressible.

All water properties are determined depending on the film temperature.

The continuity equation of incompressible fluid can be defined by:

$$\frac{\partial}{\partial x}(\rho u_i) = 0 \quad \ldots(3)$$

The thermal conductivity differs from one material to another and the energy equation can be found by [18]:

$$K_m\left(\frac{\partial^2 T}{\partial x^2}+\frac{\partial^2 T}{\partial y^2}+\frac{\partial^2 T}{\partial z^2}\right) = 0 \quad \ldots(4)$$

Although, the equation of energy can be denoted by [19]:

$$\nabla.\left(\rho h\vec{U}\right) = -p\nabla\vec{U} + \nabla(k\nabla T) + \phi + s_h \quad \ldots(5)$$

Lastly, Navier-Stokes equations of the 3D can write as customary of equations as presented in Eq. (6) [20]:

$$\begin{aligned}\nabla.\left(\rho\vec{U}\,u\right) &= -\frac{\partial p}{\partial x}+\frac{\partial \tau_{xx}}{\partial x}+\frac{\partial \tau_{yx}}{\partial y}+\frac{\partial \tau_{zx}}{\partial z}\\ \nabla.\left(\rho\vec{U}\,v\right) &= -\frac{\partial p}{\partial y}+\frac{\partial \tau_{xy}}{\partial x}+\frac{\partial \tau_{yy}}{\partial y}+\frac{\partial \tau_{zy}}{\partial z}\\ \nabla.\left(\rho\vec{U}\,w\right) &= -\frac{\partial p}{\partial z}+\frac{\partial \tau_{xz}}{\partial x}+\frac{\partial \tau_{yz}}{\partial y}+\frac{\partial \tau_{zz}}{\partial z}\end{aligned} \quad \ldots(6)$$

4. Result and Discussion

In the present study, the numerical analyses has used to depicted visibly the natural convection phenomna and therefore the temperature distribution of the operating liquid and water inside the thermosyphon loop and the container.

4.1. Time Step and mesh Independent

Because of all models in this work are under transient flow, the time step is much significant part to get perfect numerical result. The size and type of the mesh also greatly influence the results and their accuracy. Therefore, independent time and mesh tests were performed in order to verify the time-step tests and the number of mesh suitable for simulation of the geometrical model. Tables 2 and 3 show the results of these tests. According to the results shown in the tables, the process of doubling the time step and the number of mesh does not give a important influence on the results. Then, in order to reduce the operating time and avoid the high cost, the minimum number of mesh and the maximum time step for each case were used in the simulation.

Table 2. Test results of the time step independence

No.	Time step (second)	Difference water temperature (ºC)	Percentage difference (%)
1	3	34.89	
2	6	35.01	0.34
3	12	35.05	0.11

Table 3. Tests of the mesh independence

Case	Element number, (million)	Water temperature(ºC)	Percentage difference (%)
Traditional	1.9	12.05	
	3.9	12.028	0.1825
Case –A-	2.25	13.85	
	4.6	13.87	0.1442
Case –B-	2.4	13.64	
	4.9	13.6	0.293
Case –C-	2.6	13.7	
	5.3	13.75	0.3636

4.2. Numerical Calculations Validation

To demonstrate accurate results of the numerical model, boundary conditions and geometrical system were used completely similar to the experimental test device. Based on that, the water and operating liquid temperature in the storage container and at the entrance and exit of the absorber pipe for seven hours were clarified as shown in figure 6 (a-c). The figure below shows that the temperatures results for both the numerical and experimental model exhibit the same behavior trend. Also note a good covenant among numerical and experimental results.

According to figure 6 (a-c), the total difference among the numerical and experimental results are 14.52%, 11.23% and 14.2% for the water and the operating liquid temperature at the tank and outlet and inlet of absorber pipe respectively. The small difference among the numerical and experimental results is due to the thermal losses that happen in the experimental test, which are hard to controller, as well as the lacking accuracy of the measuring devices.

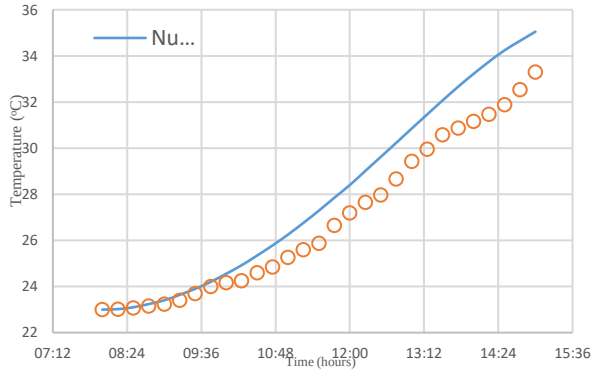

(a)

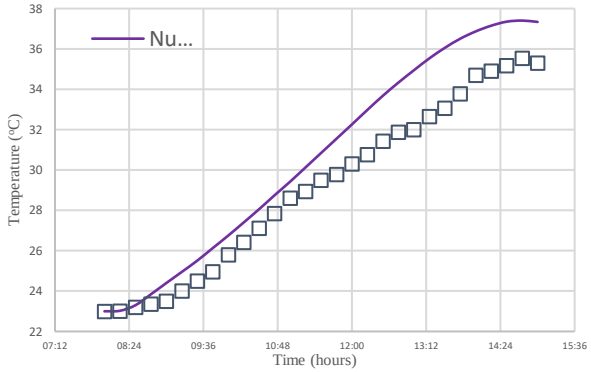

(b)

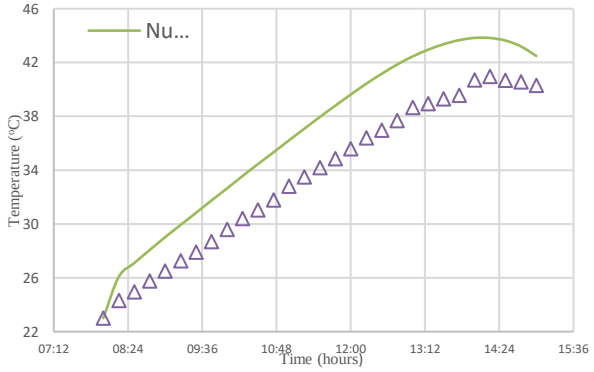

(c)

Figure 6. Contrast among numerical and experimental results for (a) Show water temperature inside the tank, (b) Show operating liquid temperature inside the entrance of absorber pipe and (c) Show operating liquid temperature inside the exit of absorber tube.

4.3. Effect of Absorber Pipe Geometry

To rise the absorption area and keeping the same volume of operating liquid compared to the conventional case, the influence of add fins about the absorption tube was studied in this sector. So, the work objectives to study the influence of added fins about the absorber tube on the thermal performance of the thermo-siphon. Details of these fins are mentioned early in section 3.1. Figure (7) show the temperature distribution of the operating liquid and water in thermo-siphon and the storage of a) for the traditional case, b) for case -A-, c) for case -B- and d) for case -C- at maximum heat flux that happens at 1:00 PM. As is seeming in figure (7) (a- d), the temperature of operating liquid inside the riser tube remains hotter compared to down-comer for both shapes. Moreover, the temperature of water within the storage container and operating liquid in the thermo-siphon loop for cases A, B and C is greater compare to traditional case. Moreover, the mean water temperature in the storage container for conventional model, case (-A-), case (-B-) and, case (-C-) is (30.85^{o}C), (32.1^{o}C), (32.06^{o}C), and (32.08^{o}C) respectively. While, the mean operating liquid temperature for traditional model, case (-A-), case (-B-) and case (-C-) were (38.69^{o}C), (41.3^{o}C), (40.3^{o}C), and (41.1^{o}C) respectively. The reason behind increase of temperatures because of increased the absorption area because of adding ring fins about the absorber tube.

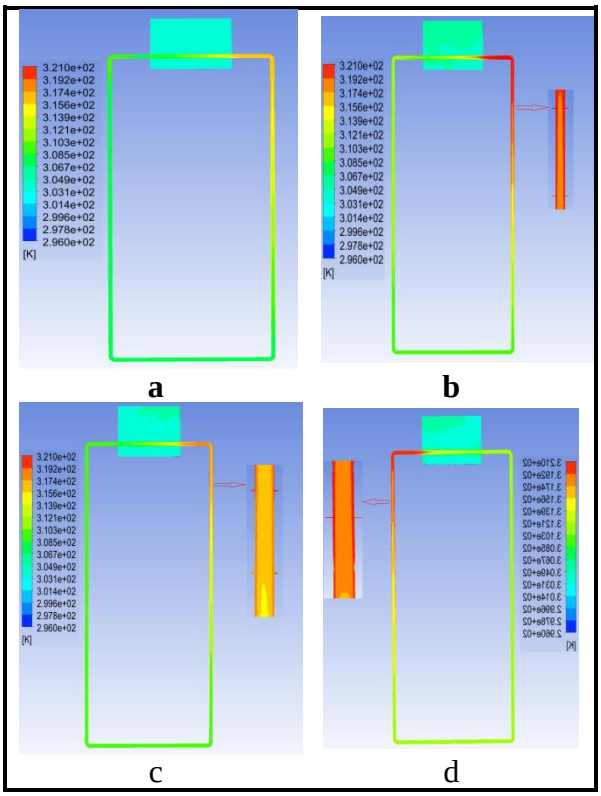

Figure 7. Show temperature contour of a operating liquid inside thermo-syphon loop, and water in the tank (a) For conventional model, b) case -A-, c) case -B- and d) case -C-.

Figure (8) show the flow velocity variations of the water in the storage tank and operating fliquid in thermosyphon closed loop, at maximum heat flux that happens 1:00 PM. The upper of the riser pipe has a much higher flow velocity. This due to the hot water rising up in a cross section of the absorber tube thereafter move towards the up riser. Moreover, it is notice that the speed inside the absorber pipe is higher in the cases of the adding fins compared to the inserting cases due to less friction and a small flow diameter. The velocity of the operating liquid increases greatly due to higher the heat input to the thermo syphon.

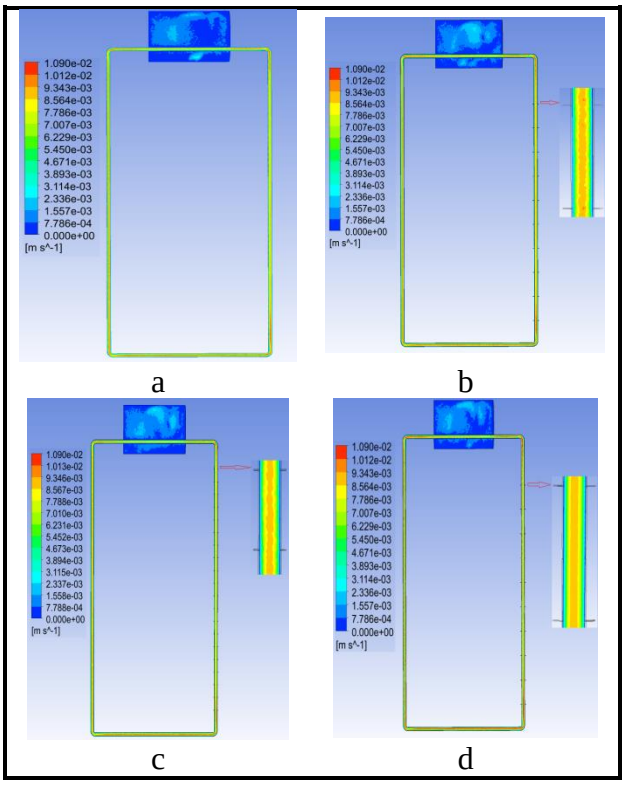

Figure 8. velocity contour inside a tank and thermo syphon loop (a) traditional model, b) case -A-, c) case -B- and d) case -C-.

To inspect the impact of add fins about the absorbent pipe on the thermosyphon performance, the difference of the water and operating liquid in the tank and in the entrance and exit of the absorber tube for two cases are compared for different of heat flux as presented in figure (9) (a-c). It is noted that the temperature of both water in the storage container and the operating liquid at the inlet and exit of the absorber tube of case -A- was greater compare to traditional model. However, the water and the operating liquid temperature in the tank and at the entrance and exit of the absorber tube for case -A- are approximately 13%, 12.037% and 15.6% higher compared to conventional model for seven hours. The reason for the increment is due to the increase of the absorption area of resulting from adding the ring fins to the absorber pipe.

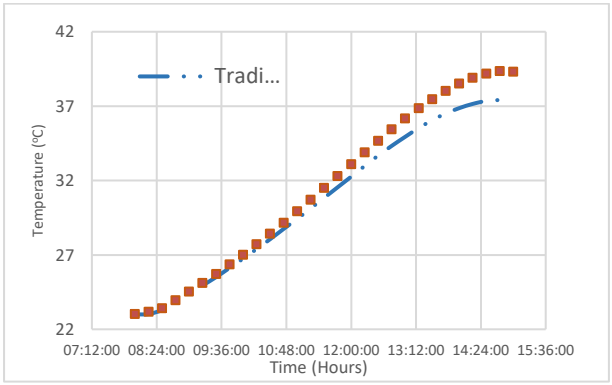

(a)

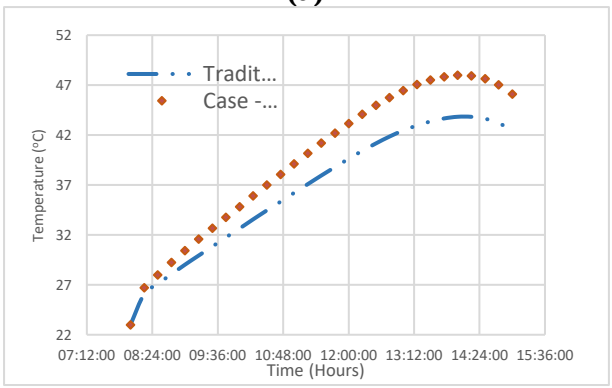

(b)

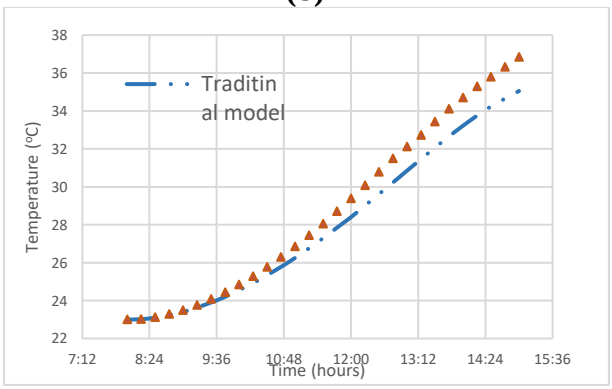

(c)

Figure 9. Difference of temperature distribution of (a) For the operating liquid at the entrance of absorber tube, (b) the operating liquid at the exit of absorber tube and (c) water in the storage container at different heat flux.

The effect of added twenty Fins on each of the operating liquid and tank temperature can be notice clearly from figure (10) (a-c) respectively. This figure shows that the behavior for both temperatures of operating liquid in the thermosyphon and of water temperature in the tank for case (B) is similar to behavior of case (A). The maximum enhancement for new model case (B) is 11.11%, 11% and 11.65% for operating liquid inlet of absorber pipe, operating liquid exit of absorber pipe, and the water in a tank as compared to traditional model.

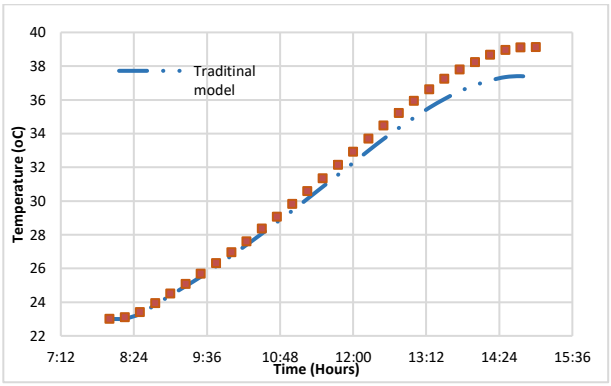

(a)

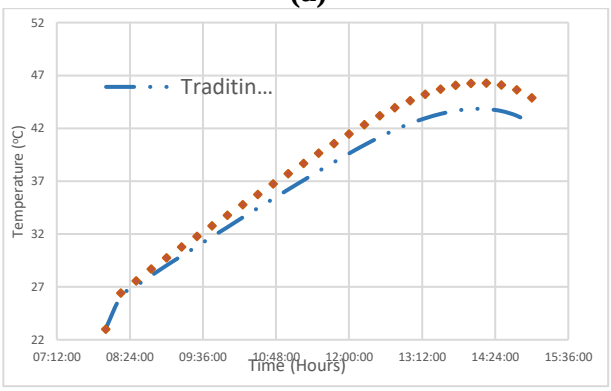

(b)

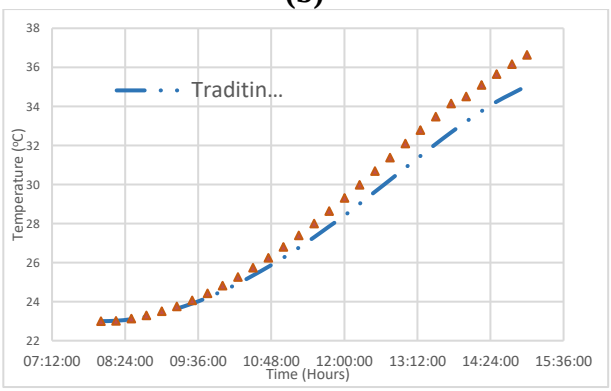

(c)

Figure 10. Temperature distribution with versus time (a) For operating liquid at the entrance of absorber tube, (b) operating liquid at the exit of absorber tube and (c) water in the storage tank with 20 fins.

Figure (11) shows the difference in operating liquid water temperature inside a thermosyphon and the tank with respect to time when using 10 fins and 10 grooves. Creating grooves in the absorption tube reduces the thickness of the tube and increases the surface area, as this improves the heat collection process. Through the figure, it found that the maximum temperature

alteration developed by the thermosyphon for case –C- as compared to conventional model is 20.3%, 17.76% and 12.04% for operating liquid entrance of riser pipe, operating liquid exit of riser pipe, and the water in a tank.

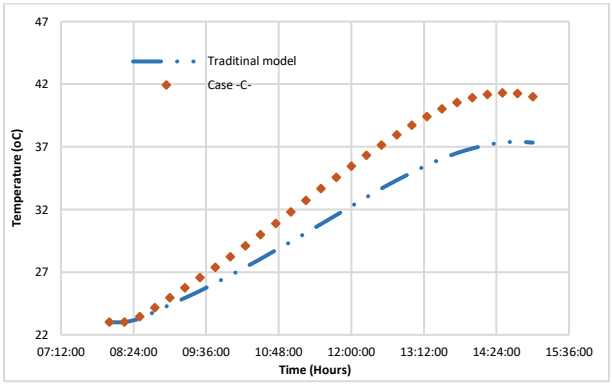

(a)

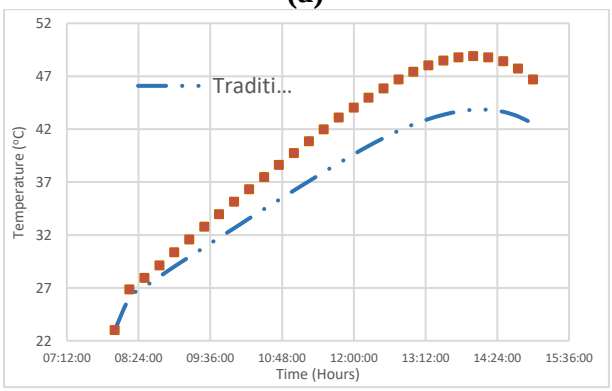

(b)

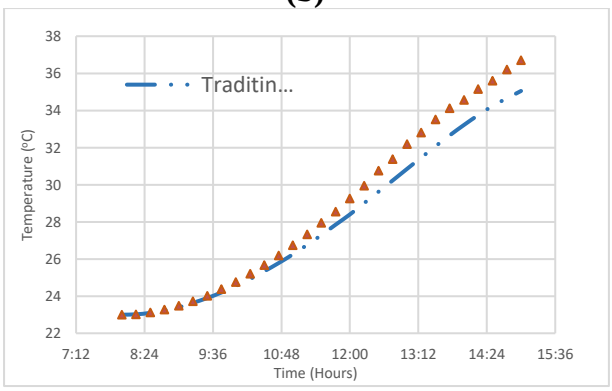

(c)

Figure 11. Temperature distribution against the time for (a) operating liquid at entrance of absorber tube, (b) operating liquid at the exit of absorber tube and (c) water in the tank with 10 fins and 10 grooves.

It can be concluded from the previous cases that they gave close improvement rates, and this indicates that the difference in the added surface area (fins) has a higher heat transfer effect as shown in table (4).

Table 4. The effect of added fins on the system performance.

fins	The operating liquid temperature of at exit of the riser pipe (°C)	Temperature of water inside the tank (°C)
10 fins case-A-	46.1	36.85
20 fins case-B-	44.89	36.64
10 fins with 10 groove case-C-	46.68	36.7

From table (4) it can be concluding that maintaining of the same absorption area in case of any enhancement on such systems is very important. Case-A- achieved highest water temperature in a tank as compared to other cases. Heating the water in a tank is the main purpose of these systems. Consequently, case (A) can be considering the best case among the cases under study. Since the use of 10 fins is the best among the three previous cases.

5. Conclusions

Comparative study between experimental and numerical results for three models of thermosyphon with a conventional model was conducted. A convergence of experimental and numerical results is observed as all tests were performed under a transient flow. It was found through the numerical results that the case-A- is the best. The following conclusions are summarized:

1. Maximum difference among experimental and numerical results discovery of the conventional model were 14.52%, 14.21% and 11.23% for the water temperature within the tank and operating liquid temperature within the entrance and exit of absorber pipe respectively.
2. It is found that all developed models under study have greater thermal performance than conventional model. This performance improvement is clearly notice through the increase of the operating liquid temperature in thermosyphon and water temperature within the tank respectively.

3. Among all cases under study case-A- is found as the best thermal response case. For this case, the water and operating liquid temperature within the tank and the entrance and the exit of the absorber tube are greater by approximately 13%, 12.03% and 15.6% compared to conventional model.

Nomenclature

Pr	Prandtl number
T	temperature, K
$T_{w,t}$	tank temperature, K
$T_{w,i}$	Inlet water temperature of riser pipe,K
$T_{w,o}$	Outlet water temperature of riser pipe,K
q	Heat flux w/m2

Greek symbols

ν	Kinematic viscosity, m2/s
ρ	Density, kg/m3
μ	Dynamic viscosity, N•s/m2
I_T	Intensity of solar radiation
δ	inclination angle
ε	Earth's orbit correction factor
θ	Tilt angle of thermo-syphon
τ	Atmospheric transmittance
ω	Sun hour angle
∝	local latitude

6. References

1. Jones, Geoffrey G., and Loubna Bouamane. (2012) *"" Power from Sunshine":* A Business History of Solar Energy." Harvard Business School Operating Paper Series.
2. Duffie, John A., and William A. Beckman. Solar engineering of thermal processes. New York: Wiley, 1991.
3. B. Freegah, et al (2014) *"Effect of the shape of connecting pipes on the performance output of a closed-loop hot water solar thermosyphon,".*
4. M. S. Manjunath, K. Vasudeva Karanth, and N. Yagnesh Sharma, (2011) *"Three dimensional numerical analysis of conjugate heat transfer for enhancement of thermal performance using finned tubes in an economical unglazed solar flat plate collector,"* Proc. World Congr. Eng. 2011, WCE 2011, vol. 3, no. July, pp. 2245–2249.
5. P. N. Shrirao, S. S. Pente, and A. N. Mahure, *"Comparative Thermal Analysis of a Flat Plate Solar Collector using Aerofoil Absorber Tube with Conventional Circular Absorber Tubes,"* Int. J. basic Appl. Res., vol. 7, no. 12, pp. 98–107.
6. M. Balachandar and A. Narendran, (2016) *"Experimental Investigation of Solar Flat Plate Collector with Inner Grooved Copper Tube,"* Int. J. Eng. Res., vol. V5, no. 09, pp. 695–700,.
7. H. M. S. Hussein, H. H. El-Ghetany, and S. A. Nada (2006) *"Performance of wickless heat pipe flat plate solar collectors having different pipes cross sections geometries and filling ratios,"* Energy Convers. Manag., vol. 47, no. 11–12, pp. 1539–1549,.
8. J. V Bute and S. C. Kongre, (2015) *"EXPERIMENTAL INVESTIGATION OF A SOLAR FLAT PLATE COLLECTOR,"* Int. Eng. J. Res. Dev., vol. 2, no. 5, pp. 36–46,.
9. K. Yao, T. Li, H. Tao, J. Wei, and K. Feng, "Performance Evaluation of All-glass Evacuated Tube Solar Water Heater with Twist Tape Inserts Using CFD," Energy Procedia, vol. 70, pp. 332–339, 2015.
10. R. Herrero Martin, A. G. Pinar, and J. P. Garcia, (2011) *"Experimental Heat Transfer Research in Enhanced Flat-Plate Solar Collectors,"* Proc. World Renew. Energy Congr. – Sweden, 8–13 May, 2011, Linköping, Sweden, vol. 57, pp. 3844–3851,

11. R. Khargotra, S. Dhingra, R. Chauhan, and T. Singh, (2018) *"Performance investigation and comparison of different turbulator shapes in solar water heating collector system,"* AIP Conf. Proc., vol. 1953,.
12. C. Sharma, (2014) *"Experimental Study on an Enhanced Performance Solar Water Heater,"* pp. 20–25,
.13. B. K. Ameen, (2015) *"Heat Transfer Enhancement of Flat Plate Solar Collectors for Water Heating in Iraq Climatic Conditions,"* Al-Nahrain Univ. Coll. Eng. J., vol. 18, no. 2, pp. 259–272,.
.14. A. Hobbi and K. Siddiqui (2009) *"Experimental study on the effect of heat transfer enhancement devices in flat-plate solar collectors,"* Int. J. Heat Mass Transf., vol. 52, no. 19–20, pp. 4650–4658,.
15. Hu, Jiangtao, et al. (2002*) "Overlay Grid Based Geometry Cleanup."* IMR..
16. Aung, N.Z. and S. Li, Numerical investigation on effect of riser diameter and inclination on system parameters in a two-phase closed loop thermosyphon solar water heater. Energy Conversion and Management, 2013. 75: p. 25-35.
17. Handbook, A., 1985 Fundamentals. American Society of Heating, Refrigerating, and Air Conditioning Engineers, Inc., Atlanta, Georgia, 1985.
18. J. Blazek, Computational Fluid Dynamics: Principles and Applications.
19. K.A. Hoffmann, S.T. Chiang, Comput. Fluid Dyn. (2000).
20. B.R. Munson, D.F. Young, T.H. Okiishi, Fundamentals of Fluid Mechanics, John Wiley & Sons. Inc., New York, 1994, p.2.